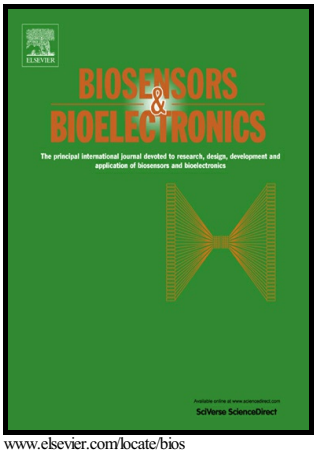

www.elsevier.com/locate/bios

Ultrasensitive electrochemical detection of tumor cells based on multiple layer CdS quantum dots-functionalized polystyrene microspheres and graphene oxide – polyaniline composite

Jidong Wang, Xiaoyu Wang, Hengshan Tang, Zehua Gao, Shengquan He, Jian Li, Shumin Han

PII: S0956-5663(17)30535-3
DOI: http://dx.doi.org/10.1016/j.bios.2017.07.077
Reference: BIOS9910

To appear in: *Biosensors and Bioelectronic*

Received date: 5 June 2017
Revised date: 16 July 2017
Accepted date: 31 July 2017

Cite this article as: Jidong Wang, Xiaoyu Wang, Hengshan Tang, Zehua Gao, Shengquan He, Jian Li and Shumin Han, Ultrasensitive electrochemical detection of tumor cells based on multiple layer CdS quantum dots-functionalized polystyrene microspheres and graphene oxide – polyaniline composite, *Biosensors and Bioelectronic,* http://dx.doi.org/10.1016/j.bios.2017.07.077

Ultrasensitive electrochemical detection of tumor cells based on multiple layer CdS quantum dots-functionalized polystyrene microspheres and graphene oxide – polyaniline composite

Jidong Wang,[*,a] Xiaoyu Wang,[a] Hengshan Tang,[a] Zehua Gao,[a] Shengquan He,[a] Jian Li,[a] Shumin Han*,[a,b]

[a] Hebei Key Laboratory of Applied Chemistry, School of Environmental and Chemical Engineering, Yanshan University, Qinhuangdao 066004, China

[b] State Key Laboratory of Metastable Materials Science and Technology, Yanshan University, Qinhuangdao 066004, China

Xiaoyu Wang E-mail:793451503@qq.com; Hengshan Tang E-mail: 1262754703@qq.com;

Shengquan He E-mail:2252089989@qq.com; Zehua Gao E-mail:641830880@qq.com;

Jian Li E-mail: lijianbio@ysu.edu.cn

***Corresponding author**

Jidong Wang E-mail: wangjidong@ysu.edu.cn; Tel.: +86-335-804-6508;

Shumin Han E-mail: hanshum1n@163.com; Tel.: +86-335-807-4648.

Address: College of Environmental and Chemical Engineering, Yanshan University, Qinhuangdao 066004, China

Abstract

In this work, a novel ultrasensitive electrochemical biosensor was developed for the detection of K562 cell by a ~~dual~~ signal amplification strategy based on multiple layer CdS QDs functionalized polystyrene microspheres(PS) as bioprobe and graphene oxide(GO) -polyaniline(PANI) composite as modified materials of capture electrode. Due to electrostatic force of different charge, CdS QDs were decorated on the surface of PS by PDDA (poly(diallyldimethyl-ammonium chloride)) through a layer-by-layer(LBL) assemble technology, in which the structure of multiple layer CdS QDs increased the detection signal intensity. Moreover, GO-PANI composite not only enhanced the electron transfer rate, but also increased tumor cells load ratio. The resulting electrochemical biosensor was used to detect K562 cells with a lower detection limit of 3 cells mL^{-1} (S/N=3) and a wider linear range from 10 to 1.0×10^7 cells mL^{-1}. This sensor was also used for mannosyl groups on HeLa cells and Hct116 cells, which showed high specificity and sensitivity. This ~~dual~~ signal amplification strategy would provide a novel approach for detection, diagnosis and treatment for tumor cells.

Keywords: Signal amplification; Layer-by-layer assemble; CdS QDs functionalized polystyrene microspheres bioprobe; GO-PANI composite; Tumor cells detection; Electrochemical biosensor

1. Introduction

K562 was usually chosen to detect human chronic myelogenous leukemia (CML) because it was a type of most uncontrolled and destructive human CML cell line. Different from normal cell line, K562 cells associated with the changes in the expression of cell surface carbohydrates, for example mannosyl groups et al. Therefore, the detection methods based on the precise molecular recognition for the carbohydrates on K562 cells surface, would propose an efficient and accurate approach for the clinical diagnostics of CML. Concanavalin A (Con A) as a novel lectin, has been used to specifically recognize the mannosyl groups on cell surface with excellent specificity and high affinity.

At the moment, on analytical technique and device of K562 cells detecting, including fluorescence (Wu et al. 2003), electrochemical impedance spectroscopy (Wang et al. 2011), mass spectrometry (Li et al. 2002), flow cytometry (Pitsillides et al. 2011), and a number of indirect detection methods (Liu et al. 2013a; Zhou et al. 2016), have been developed. However, these methods usually required relatively expensive equipment, hypertoxic materials, time-consuming. Although promising, it's critical that these techniques often suffered from the lack of specificity, stability and sensitivity. Especially, the coupling of the nanostructured biointerfaces in these sensors showed low affinity and activity. In early stages, due to the presence of biomarkers or tumor cell with low concentration, these analytical techniques would not achieve highly sensitivity with satisfaction. Compared with these conventional analysis techniques, the electrochemical (EC) methods, is a popular detection technique due to their operational simplicity, high sensitivity and low background (Dong et al. 2016; Feng et al. 2016; Su et al. 2014). Various electrochemical strategies have been investigated, especially in the use of nanomaterials and carbon materials to achieved high sensitivities and preferable specificity. To explore new materials and new methods to improve sensitivity and broaden detection range, are the permanent goals of electrochemical methods for detecting tumor cell.

Graphene oxide (GO), as a two-dimensional carbon nanomaterial with high specific surface area, biocompatibility and water dispersion , has been much attention in exploiting the application in various fields (Valentini et al. 2013; Wu et al. 2012) (Du et al. 2014) (Liu et al. 2013b) (Kim et al. 2010; Sheng et al. 2012). Meanwhile, GO, with the abundant and high-density carboxyl groups, greatly improved its interface load ratio and biocompatibility in electrochemical analysis and detection (Azimzadeh et al. 2016; Han et al. 2014; Shieh and Jiang 2015). Polyaniline is a unique conductive polymer, which could stack with GO to increase its conductivity. So, the combining GO and PANI (GO-PANI) as the modified materials of electrode have also been applied to increase the load ratio and conductivity in the detection and analysis fields (da Silva et al. 2014; Fu et al. 2016; Nazari et al. 2015).

Semiconductor quantum dots (QDs) as a novel fluorescent probes due to their unique optoelectronic characters, such as large stokes shift, high quantum yield and narrow fluorescence emission(Li et al. 2015). In particular, among various QDs, CdS QDs have been applied to electrochemiluminescence (ECL) and electrochemical sensor directly (Gill et al. 2008; Jie et al.

2010; Jie et al. 2007). In a practical detection system, the materials, with multilayers, microporous structures, high surface area-to-weight ratio, and fast electron-transfer capabilities usually were assembled as media for carrying QDs by layer-by-layer (LBL) techniques. PAMAM-GO composite (Zhu et al. 2016), SWCNTs (Tu et al. 2015), mesoporous silica nanoparticles (Su et al. 2014), Fe_3O_4 magnetic nanoparticles (Sun et al. 2015) have been proved to contribute to enhance sensitivity due to their unique structure and property (Xiang et al. 2011a;Wang et al. 2012; Xiang et al. 2011b; Xie et al. 2012, Shen et al. 2014).

Herein, we present a ~~dual~~ signal amplification system based on the multiple layer CdS QDs-functionalized polystyrene microspheres (PS-$(CdS\ QDs)_n$) as signal probe and GO- PANI composite as the modified materials of electrode to construct ultrasensitive electrochemical biosensor for detecting the K562 cells. Due to the difference of charge, the PDDA (poly(diallyldimethyl-ammonium chloride) with positive charge and the CdS QDs with negative charge grew alternately by the layer-by-layer technology on the surface of PS. Con A was capped on the carrier of PS-PDDA-$(CdS\ QDs)_n$ by EDC/NHS activation to form PS-PDDA- (CdS QDs)n-Con A conjugates as the signal probe. High surface and multiple layer structure would increase the signal intensity and enhance detection sensibility. GO- PANI composite provided a large surface area and high electron transfer rate. Through the crosslinking of glutaraldehyde (GA), a great quantity of Con A was loaded on the electrode surface to capture the K562 cells. After the surface was decorated by GO-PANI-GA-Con A composite, the capture electrode possessed the high cell load rate and conductivity. Therefore, an ultrasensitive electrochemical biosensor for detecting K562 cells would be obtained. This biosensor with high specific surface area and biocompatibility showed higher sensitivity, wider detection range and lower LOD. This method has also been used to determine the surface carbohydrates of HeLa cells and Hct116 cells with satisfactory.

2. Material and methods

2.1 Materials and reagents

Graphene oxide was synthesized by the Hummers method (Dimiev and Tour 2014). Graphite, H_2SO_4, $KMnO_4$ were purchased from Sigma (St. Louis, MO, USA). K562 cells line was obtain

from SincereLion Technology (beijing) Co. Ltd. and were cultivated according to the literature (Ge et al. 2015). Polyaniline (PANI) was obtained from Alfa Aesar (China chemical co., Ltd). N -(3- (dimethylamino)- propyl)- N′- ethylcarbodiimide hydrochloride (EDC) N-hydroxysulfosuccinimide (NHS), were purchased from Sigma-Aldrich. Mercuric nitrate was bought from Xiya Reagent (Shandong, China). Concanavalin A was purchased from Sangon Biotech Co., Ltd (Shanghai, China). nine hydrated sodium sulfide, cadmium chloride, sodium citrate, 3-mercaptopropionic acid (MPA), poly(diallyldimethyl-ammonium chloride) (PDDA), polystyrene microspheres (PS), potassium chloride, calcium chloride, manganese chloride, bovine serum albumin (BSA), glutaraldehyde (GA), nitric acid (65%), potassium ferrocyanide, sodium acetate, glacial acetic acid and phosphate buffer solution (PBS, 10 mM, pH=7.2-7.4) were obtained from Aladdin science and technology (China) Co., Ltd (Shanghai), including. All reagents were analytical grade without further purification.

2.2 Apparatus and electrochemical measurement

UV-Vis absorption spectroscopy and fluorescence spectrum measurements were recorded on a UV-2550 (Shimadzu, Kyoto, Japan) and F-7000 (Hitachi, Tokyo, Japan). Transmission electron microscopic (TEM) and scanning electron microscopic (SEM) images were obtained by a HT7700 transmission electron microscope (Hitachi, Tokyo, Japan) and a SUPRA 55 scanning electron microscope (CarlZeiss, Germany), fluorescence microscopic image was obtained from XSP-63X fluorescence microscope (The first factory of optical instrument in Shanghai, China) respectively.fluorescence microscope, respectively.

All the Electrochemical measurements were carried out on a CHI 660E electrochemical workstation (Shanghai Chenhua instrument Co., Ltd, China) with a three-electrode system composed of a glassy carbon electrode (GCE, 3 mm in diameter) as the working electrode, a platinum electrode as counter electrode and a saturated calomel electrode (SCE) as reference electrode. Electrochemical impedance spectroscopy (EIS) and cyclic voltammetry (CV) were performed in 5 mM $K_3Fe(CN)_6$ / $K_4Fe(CN)_6$ (0.1 M KCl) as the supporting electrolyte. The anodic stripping voltammetry (ASV) detection involved in a 30 min electrodeposition at -1.2 V, and using a square-wave voltammetry, scanning the potential from -1.1 to -0.2 V with potential step of 4 mV,

frequency of 25 Hz, and amplitude of 25 mV.

2.3 Preparation of PS-(CdS)n-Con A Conjugates

Water soluble MPA-capped CdS QDs were synthesized via a facile one-pot methods at room temperature. First 0.8 mmol cadmium chloride, 0.4 mmol sodium citrate, 0.4mmol MPA, 25 ml distilled water were load into the flask in sequence with vigorous stirring and pH value was adjusted to 9 with 1 M NaOH. With the addition of 0.04 mol/L Na_2S under the stirring, the white turbid solution became colorless and transparent instantaneously. Stirring constantly over one night, the solution became pale green. The final MPA-capped CdS QDs solution was washed with absolute ethanol and distilled water for three times, and then stored in dark at 4 ℃.

50 μL polystyrene microspheres (PS, 5%) were immersed into 1 mL PDDA (0.2 wt %) solution and sonicated for 10 min. After washing three times by distilled water and centrifuging, 1mL MPA-capped CdS QDs (6.1×10^{-6} mol/L) were added in the above PS-PDDA solution and stirred for 12 h. The product of PS-(CdS)n was obtained using this LBL technology by repeating the above two procedures alternately. Finally, the PS-(CdS)n was activated in 500 μL mixture solution of EDC (20 mg/mL) and NHS (10 mg/ml) (V_1:V_2=1:1) at 37 ℃ for 1 h. 500 μL Con A solution was dropped into the active solution of PS-(CdS)n crosslinking 1 h. The product was obtained after washing three times by distilled water and dispersed in 500 μL PBS.

2.4 Fabrication of the biosensor

The fabrication and detection procedure of electrochemical biosensor was illustrated in Scheme 1. A GCE (3 mm) was firstly polished with 0.3 and 0.05 μm α-Al_2O_3 powder and sonicated in absolute alcohol and distilled water, respectively, and then drying with N_2 at room temperature. 10 μL GO (1 mg/mL) solution was dropped on the GCE and dried at room temperature for 8 h. Then, 10 μL PANI (0.25 mg/mL) was cast on the surface of GO coated working electrode to connect with GO by π-π stacking. After 2 h of incubation, the electrode was washed by PBS (10 mM, pH=7.2-7.4). Then, the electrode was immersed in 10 μL GA solution (2.5%) for 1.5 h at room temperature, and the GA was linked on the electrode by the reaction with PANI. Subsequently, 10 μL 1mg/mL Con A, which had been activated for 6 h in PBS (10 mM,

pH=7.2-7.4) containing Ca^{2+} and Mn^{2+} (Bucur et al. 2004)) was cast on the surface of GCE-GO-PANI-GA electrode and incubated for 2 h. Finally, 1% BSA was used to block non-specific sites and the nonspecific adsorptions were washed out by PBS solution.

The capture electrode GCE-GO-PANI-GA-Con A was immersed in K562 cells solution with different concentration for 30 min. After the adhesive cells on electrode were rinsed by the salt balance PBS, 5 μL probe solution, PS-(CdS)n-Con A conjugates were dropped onto the capture electrode, then washed with the buffer and stored for detection.

Scheme 1.

2.5 The sensing procedure for detection of K562

In order to determine Cd^{2+} in sensing system, the as-assemble electrode was immersed into HNO_3 (200 μL, 0.1 M) solution for 2 h to dissolve the QDs. Then, the solution was mixed with acetate buffer (HAc-NaAc buffer, 4.8 mL, 0.2 M, pH 5.2) containing 20 μg/mL Hg^{2+} in order to detect metal ions by ASV. The electrode position in this method was at −1.2 V and standing for 30 min. Square-wave voltammetric waveform was recorded by stripping from −1.1 to 0.5 V, in which the potential step was 4 mV, the frequency was 25 Hz, and the amplitude was 25 mV. Due to a positive relationship between Cd^{2+} content and the K562 concentration, detection of K562 was achieved using the strong and sharp peak of Cd^{2+} at -0.72 V in ASV (Liu et al. 2015).

3. Results and discussion

3.1 Characterization of CdS QDs and PS-(CdS QDs)n probe

The UV-vis absorption and PL spectra of MPA-capped CdS QDs were recorded in Fig. 1A. The distinct exciton absorption appeared at 323 nm and the strong fluorescence emission peak at 494 nm, which indicated the Stokes shift was about 171 nm. The large Stokes shift showed that a lot of dangling bonds or flaws on the surface of QDs, which would be benefited for connecting with polyelectrolyte, such as PDDA. According to the Peng's empirical formula (Yu et al. 2004): $D = (-6.6521 \times 10^{-8})\lambda^3 + (1.9557 \times 10^{-4})\lambda^2 - (9.2352 \times 10^{-2})\lambda + 13.29$, we could calculate that the size of CdS QDs was about 1.6 nm. Among the equation, D (nm) is the diameter of CdS QDs and λ (nm) is the excitonic absorption peak position. TEM analysis of as-synthesis QDs also indicated

that these QDs had spherical shapes and the average size was about 1.6 nm as shown in Fig. 1B, which was consistent with the calculation of above empirical equation.

The morphology of PS, PS-PDDA, and PS-(PDDA-QDs)$_n$ was investigated by TEM as shown in Fig. 1C, D and E. The PS exhibited uniform and smooth surface. The diameter of PS is about 5 μm. TEM image in Fig. 1D illustrated that a few protruding portions appeared on the PS surface after the monolayer PDDA coated by electrostatic attraction. CdS QDs were assembled on the surface PS-PDDA by the same principle, as Fig. 1E. CdS QDs were distributed on the surface of PS-PDDA composition. A series of changes demonstrated that using this LBL technology, the multilayer self-assembly of PS-(PDDA-QDs)n composite would be obtained to increase the loader quantity of QDs for the signal amplification. The confocal fluorescent images of the prepared sample were exhibited in Fig. 1F and Fig. 1G. As reference, in the fluorescent microscopic image under visible light (Fig. 1F), PS-(CdS QDs)n conjugates showed a monodisperse and ordered array without any color. When the fluorescent microsphere was excited by laser, whose wavelength was 365 nm, as the Fig. 1G, the similar the region confocal fluorescent imaging exhibited green fluorescent. The microscopic observation also suggested that CdS QDs were assembled on the PS surface.

Fig. 1

3.2 Characterization of biosensor

During the construction process of electrochemical sensor, the morphology characters of electrode surface were investigated by SEM (Fig. S1). GO as the substrate material, usually showed a relatively flat structure, which was suitable for the modification of GCE because of its large surface area, π–π conjugate structure and good conductivity. As Fig. S1A showed, an ultra-thin paper-like morphology with slight wrinkle coated on GCE, which demonstrated that the GO possessed good dispersion and high compatibility. When PANI was assembled onto the electrode (Fig. S1B), many particles appeared on the smooth surface of GCE-GO, which illustrated that PANI had connected with GO via π–π stacking. After glutaraldehyde being immobilized, the SEM image of PANI coated GCE-GO became blurring due to the form of the membrane resulted from the condensation reaction between the –CHO of GA and –NH_2 of PANI

as shown in Fig. S1C. Subsequently, Con A was immobilized on modified GCE using the link agent GA via the same way between amino group and aldehyde group (Fig. S1D). Therefore, several distinguishable assembly processes exhibited in the SEM image. (i) Through a π–π stacking, PANI and GO attached on GCE in sequence. (ii) Though amino crosslinking, Con A was immobilized on the surface of PANI. The two –CHO of GA reacted with the $–NH_2$ in both PANI and Con A. After the non-specific sites were blocked with BSA (Fig. S1E), the modified GCE was immersed in K562 cells solution with different concentration to recognize the mannosyl groups on the surface of tumor cell by Con A. As shown in Fig. S1 F, the cell particles uniform distributed on the surface of electrode.

Fig.2

Electrochemical impedance spectroscopy (EIS) and cyclic voltammetry (CV) were adopted for investigating the surface modification progress of GCE. EIS and CV were carried out in a support solution of 5 mM $[Fe(CN)_6]^{3-/4-}$ as electroactive redox probe. Electrode treatment in different stages were described in the EIS and CV of GCE as shown in Fig. 2. The semicircle diameter of EIS in high frequency region is correlation to electron-transfer resistance (R_{et}). A change in diameter reflects the blocking behavior in the modification processes of electrode which associated with a change of R_{et}. The R_{et} of bare GCE showed a small value (Fig. 2A curve a) for the free electron transfer process, and the peak current of CV was distinct (Fig. 2B curve a) Compared with the bare GCE, due to introducing oxygen atoms to form the C=O covalent bonds, GO significantly blocked the interfacial electron transfer, which exhibited a much higher R_{et} in the ESI (Fig. 2A curve b), while the peak current of CV decreased (Fig. 2B curve b). But when the PANI was coated on the GCE-GO, a lower R_{et} was shown in the ESI spectrum (Fig. 2A curve c) and the peak current of CV increased (Fig. 2B curve c). Polyaniline, as a conductive polymer, PANI could greatly promote the efficiency of the electronic transfer in the interface and improved the electrical signal intensity. Dropping GA onto GCE-GO-PANI layer, R_{et} (Fig. 2A curve d) increased and the peak current of CV fell, which indicated that GA crosslink with PANI by condensation reaction between $–NH_3$ and –CHO. Subsequently, the immobilization of Con A onto the GCE-GO-PANI electrode, the R_{et} increased (Fig. 2A curve e), which indicated that electron exchange between the redox probe, $[Fe(CN)_6]^{3-/4-}$, and the modified electrode was blocked by

Con A. The peak current of CV decreased continuatively. Similarly, blocking the residual nonspecific binding sites with BSA, also led to a continual increase of R_{et} (Fig. 2A curve f). K562 cell immobilized the surface of GCE-GO-PANI-GA-Con A, which showed impedance of the GCE (Fig. 3A curves g) a great increase. The isolation between redox probe and electrode interface made R_{et} increase about twice due to the effect of steric hindrance. From what had investigated, it was testified that K562 cells had been immobilized on the surface of electrode. As expected, the peak current of CV further decreased as shown Fig. 2B curves g.

Thereby, SEM, EIS and CV disclosed each step in electrode assembly, which testified that the fabrication of electrochemical sensor for detecting K562 cells was feasible.

Fig. 3.

3.3 Optimization of experimental conditions

In order to obtain the excellent performance of electrochemical biosensor for tumor cells determination, some experimental conditions were optimized including accumulation time, accumulation potential, the layer count of self-assembly and the concentration of acetate buffer in anodic stripping voltammetry (ASV), as shown in Fig. 3. In Fig. 3A, the peak current increased with accumulation potential from -1.0 to -1.2 V. However, in the range from -1.3 to -1.4 V, the peak current decreased immediately. Under higher accumulation potential, the Cd^{2+} in buffer solution could not stack on the surface of GCE and the hydrogen was produced easily in electrode interface due to their lower over potential. Thus, -1.2 V was chosen as the accumulation potential using for K562 cells detection. In addition, in anodic stripping voltammetry, accumulation time was another parameter to affect electrochemical signal. Increasing accumulation time could enhance the stripping peak current, as showed in Fig. 3B. But a longer accumulation time, such as beyond 30 min, did not result in a higher increase for peak current, which demonstrated that the enrichment process of Cd^{2+} was almost completed. Therefore, the optimal accumulation time for stripping peak current enhancement was chosen at 30 min.

As shown in Fig. 3C, the quantity of CdS QDs which was assembled on the surface of PS affected the sensitivity of as-product biosensor. A significant peak current changed with the quantity of QDs on the surface of PS from one layer to four layers. Beyond three layers, the peak

current changed slowly because the electric repulsion of inner layer led to the loss of probe in operation. PS-$(CdS)_3$ as the basic framework of the probe was applied to the determination of K562 cells. The effect of the concentration of acetate buffer solution was also discussed as shown in Fig. 3D. The stripping peak current increased with concentration from 0.05 to 0.25 M. High concentration of acetate buffer solution did not lead the increase of response signal. So 0.2 M was chosen as the solution in the electrochemical biosensor for tumor cells detection.

Fig. 4.

3.4 Detection of K562 tumor cells

The specifically captured PS-$(CdS)_3$ signal probes were proportional to the amount of K562 cell immobilized on the electrode. Cd^{2+} ions from the probes could be detected by ASV after they were dissolved in HNO_3 solution. The oxidation peak of Cd^{2+} is at is about -0.72 V and the intensity of oxidation peak currents of Cd^{2+} is proportional to the amount of K562 cells. The different concentrations of K562 cells samples were responded to Cd^{2+} as shown in Fig. 4. The intensity of peak currents of Cd^{2+} showed a good linear relationship with the logarithm of K562 cells concentration on the electrode, whose range was from 10 to 1.0×10^7 cells mL^{-1}. The linear regression equation was $I = -1.1473+5.13673 \lg C_{cells}$ (C_{cells}, cells mL^{-1}) with a correlation coefficient of 0.9986 (n=6). The limit of detection (LOD) was 3 cells mL^{-1} (S/N=3). The reproducibility of electrochemical biosensor was evaluated by three different concentrations of K562 cells including 10^2, 10^3 and 10^4 cells mL^{-1}. The relative standard deviation (RSD) of these three assays were 8.0 %, 6.4% and 5.2%, respectively. This indicated the electrochemical biosensor that was with reproducibility and precision. The stability of this sensor was investigated by storing the PS-(CdS)n-Con A nanoprobes in the refrigerator at 4 °C. The electrochemical biosensor retained 92 % of its original response to K562 cells at the concentration of 10^6 cells mL^{-1} after a month storage. Therefore, the electrochemical biosensor showed an accurate detection for tumor cell with the low concentration, high reproducibility and stability.

Compared with previous approaches (Table 1), this electrochemical biosensor exhibited both the lower detection limit and wider linear range, which illustrated the ~~double~~ signal amplification based on the composite probe of PS-$(CdS\ QDs)_n$ and electrode modification of GO-PANI by the

layer-by-layer assembly, could realize the trace detection of K562 cells and provided an excellent platform for diagnosis and treatment of tumor cells.

Table 1

3.5 Detection of HeLa and colorectal cancer cells

In order to evaluate the selectivity and validity of this electrochemical sensing system for mannosyl groups on other tumor cells, HeLa cells and colorectal cancer cells were investigated under identical conditions as K562 cells. As shown in Fig. S2, the electrochemical signals of HeLa cells and Hct116 cells showed almost the same intensity as K562 cells, which illustrated that this biosensor could use as a common method to detect the different cancer cells by the specific recognition of mannosyl groups.

4. Conclusions

In conclusion, an ultrasensitive, ~~dual~~ signal amplification electrochemical biosensor was fabricated by the LBL assembly, in which PS-(CdS)n was as the signal probe and GO-PANI composite was used as the modified materials for capture electrode. Due to electrostatic force, the PDDA with positive charge and CdS QDs with negative charge were assembled on the surface of PS by a repeated process. The multiple layer structure increased the detection signal intensity. Moreover, GO-PANI composite not only enhanced the electron transfer rate, but also increased tumor cells load ratio, which also led to the sensitivity increased. Based on the ~~dual~~ signal amplification, the electrochemical biosensor exhibited the excellent performance. The linear range for K562 cells was from 10 to 1.0×10^7 cells mL^{-1}. The linear regression equation was $I = -1.1473+5.13673 \lg C_{cells}$ (C_{cells}, cells mL^{-1}) with a correlation coefficient of 0.9986 (n=6) and LOD was only 3 cells/mL (S/N=3). Furthermore, this electrochemical sensing system was used for mannosyl groups on HeLa cells and Hct116 cells, which also showed high specificity and sensitivity. This fabrication method of electrochemical sensor would push the progress of the basic and applied research on detecting tumor cell.

Acknowledgments

This research was supported by the Natural Science Foundation of Hebei Province (H2015203231), Youth Foundation Project supported by the Hebei Education Department of China (QN2014004), the Key Research and Development Program of Qin Huangdao (201602A110), Doctoral Fund of Yanshan University (B821).

References

Azimzadeh, M., Rahaie, M., Nasirizadeh, N., Ashtari, K., Naderi-Manesh, H., 2016. Biosensors & Bioelectronics 77, 99-106.

Bucur, B., Danet, A.F., Marty, J.L., 2004. Biosensors & Bioelectronics 20(2), 217-225.

da Silva, J.S.L., Oliveira, M.D.L., de Melo, C.P., Andrade, C.A.S., 2014. Colloids and Surfaces B-Biointerfaces 117, 549-554.

Dimiev, A.M., Tour, J.M., 2014. Acs Nano 8(3), 3060-3068.

Dong, Y.P., Zhou, Y., Wang, J., Dong, Y.Q., Wang, C.M., 2016. Talanta 146, 266-271.

Du, J., Pei, S., Ma, L., Cheng, H.-M., 2014. Advanced Materials 26(13), 1958-1991.

Feng, Y.Q., Sun, F., Chen, L.Z., Lei, J.P., Ju, H.X., 2016. Journal of Electroanalytical Chemistry 781, 48-55.

Fu, J.J., Shi, Z.Z., Li, M., Wang, Y.Y., Yu, L., 2016. Journal of Nanomaterials.

Ge, L., Su, M., Gao, C.M., Tao, X.T., Ge, S.G., 2015. Sensors and Actuators B-Chemical 214, 144-151.

Gill, R., Zayats, M., Willner, I., 2008. Angewandte Chemie-International Edition 47(40), 7602-7625.

Han, H.S., Seol, H., Kang, D.H., Ahmed, M.S., You, J.-M., Jeon, S., 2014. Sensors and Actuators B-Chemical 204, 289-296.

Hao, C., Ding, L., Zhang, X., Ju, H., 2007. Analytical Chemistry 79(12), 4442-4447.

Jie, G., Liu, P., Wang, L., Zhang, S., 2010. Electrochemistry Communications 12(1), 22-26.

Jie, G.F., Liu, B., Pan, H.C., Zhu, J.J., Chen, H.Y., 2007. Analytical Chemistry 79(15), 5574-5581.

Kim, Y.-R., Bong, S., Kang, Y.-J., Yang, Y., Mahajan, R.K., Kim, J.S., Kim, H., 2010. Biosensors & Bioelectronics 25(10), 2366-2369.

Li, J., Zhang, Z., Rosenzweig, J., Wang, Y.Y., Chan, D.W., 2002. Clinical chemistry 48(8), 1296-1304.

Li, L., Liu, J., Yang, X., Peng, Z., Liu, W., Xu, J., Tang, J., He, X., Wang, K., 2015. Chemical Communications

51(76), 14357-14360.

Liu, H., Xu, S., He, Z., Deng, A., Zhu, J.-J., 2013a. Analytical Chemistry 85(6), 3385-3392.

Liu, H.Y., Lou, Y.B., Zhou, F., Zhu, H., Abdel-Halim, E.S., Zhu, J.J., 2015. Biosensors & Bioelectronics 71, 249-255.

Liu, J., Cui, L., Losic, D., 2013b. Acta Biomaterialia 9(12), 9243-9257.

Nazari, M., Kashanian, S., Rafipour, R., 2015. Spectrochimica Acta Part a-Molecular and Biomolecular Spectroscopy 145, 130-138.

Pitsillides, C.M., Runnels, J.M., Spencer, J.A., Zhi, L., Wu, M.X., Lin, C.P., 2011. Cytometry Part A 79A(10), 758-765.

Qiu, Y., Wen, Q., Zhang, L., Yang, P., 2016. Talanta 150, 286-295.

Shen, S., Zhao, B., Wang, H., Li, Z., Qu, G., Guo, Z., Zhou, T., Song, W., Wang, X., Ruan, W., 2014. Colloids and Surfaces a-Physicochemical and Engineering Aspects 443, 467-472.

Sheng, Z.-H., Zheng, X.-Q., Xu, J.-Y., Bao, W.-J., Wang, F.-B., Xia, X.-H., 2012. Biosensors & Bioelectronics 34(1), 125-131.

Shieh, Y.-T., Jiang, H.-F., 2015. Journal of Electroanalytical Chemistry 736, 132-138.

Su, M., Liu, H., Ge, L., Wang, Y.H., Ge, S.G., Yu, J.H., Yan, M., 2014. Electrochimica Acta 146, 262-269.

Sun, Z.H., Wang, W.H., Wen, H.B., Gan, C.F., Lei, H.T., Liu, Y.J., 2015. Analytica Chimica Acta 899, 91-99.

Tu, W., Fang, X., Lou, J., Dai, Z., 2015. Analyst 140(8), 2603-2607.

Valentini, L., Bon, S.B., Kenny, J.M., 2013. Acs Applied Materials & Interfaces 5(9), 3770-3775.

Wang, W., Foley, K., Shan, X., Wang, S., Eaton, S., Nagaraj, V.J., Wiktor, P., Patel, U., Tao, N., 2011. Nature Chemistry 3(3), 249-255.

Wang, Y., Yuan, R., Chai, Y.Q., Yuan, Y.L., Bai, L.J., 2012. Biosensors & Bioelectronics 38(1), 50-54.

Wu, X., Liu, H., Liu, J., Haley, K.N., Treadway, J.A., Larson, J.P., Ge, N., Peale, F., Bruchez, M.P., 2003. Nature biotechnology 21(1), 41-46.

Wu, Z.-S., Zhou, G., Yin, L.-C., Ren, W., Li, F., Cheng, H.-M., 2012. Nano Energy 1(1), 107-131.

Xiang, Y., Zhang, H.X., Jiang, B.Y., Chai, Y.Q., Yuan, R., 2011a. Analytical Chemistry 83(11), 4302-4306.

Xiang, Y., Zhang, Y.Y., Jiang, B.Y., Chai, Y.Q., Yuan, R., 2011b. Sensors and Actuators B-Chemical 155(1),

317-322.

Xie, S.B., Yuan, R., Chai, Y.Q., Bai, L.J., Yuan, Y.L., Wang, Y., 2012. Talanta 98, 7-13.

Yu, W.W., Qu, L.H., Guo, W.Z., Peng, X.G., 2004. Chemistry of Materials 16(3), 560-560.

Zhou, S., Wang, Y., Zhu, J.-J., 2016. Acs Applied Materials & Interfaces 8(12), 7674-7682.

Zhu, Q., Cai, F.D., Zhang, J., Zhao, K., Deng, A.P., Li, J.G., 2016. Biosensors & Bioelectronics 86, 899-906.

Figure Captions

Scheme 1. Schematic representation for the electrochemical detection of K562 based on multiple electrostatic self-assembly probes.

Fig. 1. The UV-Via and PL spectrum of CdS QDs (A) and TEM images (B) CdS QDs, (C) PS, (D) PS-PDDA and (E) PS-PDDA-QDs. The fluorescence microscope images of PS-$(PDDA\text{-}QDs)_3$ (F) under visible light irradiation. (G) under ultraviolet light irradiation(365 nm)

Fig. 2. Representative EIS and CV of sensor establishment process, (a) bare GCE, (b) GCE-GO, (c) GCE-GO-PANI, (d) GCE-GO-PANI-GA, (e) GCE-GO-PANI-GA-Con A, (f) GCE-GO-PANI-GA-Con A-BSA, (g) GCE-GO-PANI-GA-Con A-BSA-K562 cells. The frequency range: 0.1Hz – 100k Hz. The CV scan rate: 100 mV s^{-1}.

Fig. 3. The effect of (A) accumulation potential, (B) accumulation time, (C) the layer count of self-assembly, (D) the concentration of acetate buffer in ASV.

Fig. 4. (A) ASV of the biosensor for different concentration of K562 cells. (B) The relationship of electrochemical signal and cell concentration. The range of K562 cell concentration is from 0 to 10^7 cells ml-1. The illustrated error bars represent the standard error of three independent measurements.

Table 1 Comparison of analytical properties of different tumor cells.

method	cells	LOD(cell ml^{-1})	Liner	Reference
Electrochemical	K562	1000	5×10^3–5×10^6	(Hao et al. 2007)
ECL	K562	500	5×10^2–5×10^6	(Ge et al. 2015)
ECL	MCF-7	12	12–1.2×10^6	(Qiu et al. 2016)
Electrochemical and Fluorescence	CCRF-CEM	50	1×10^2–1×10^6	(Liu et al. 2013a)
Electrochemical	K562	3	10–1×10^7	This work

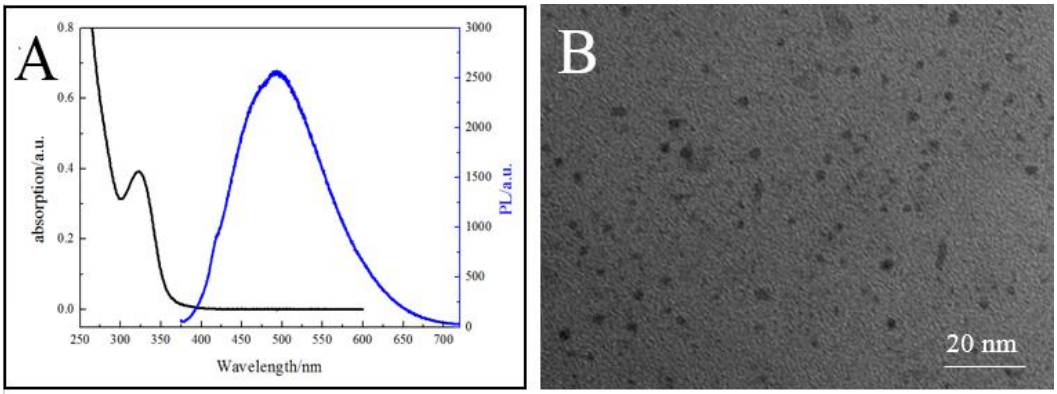

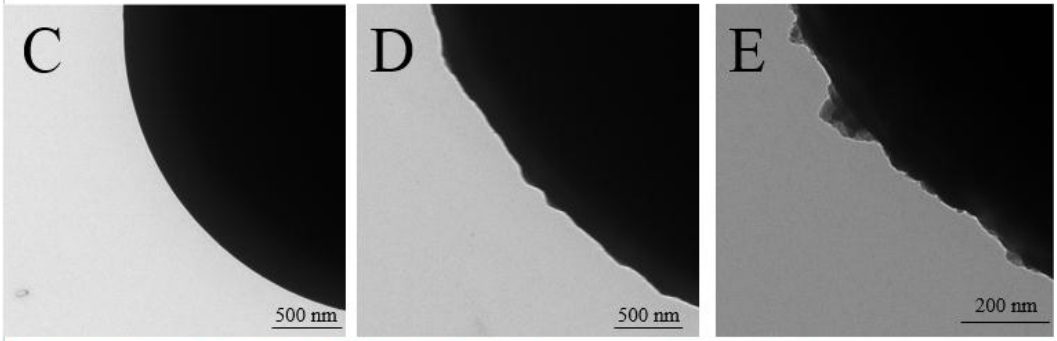

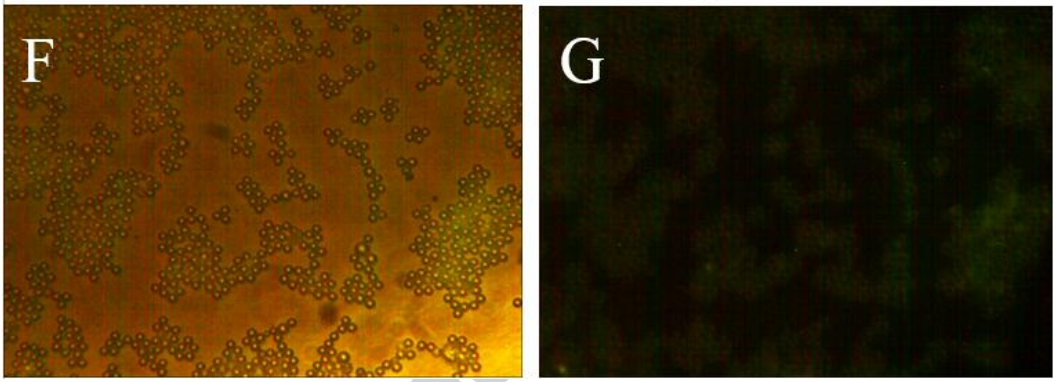

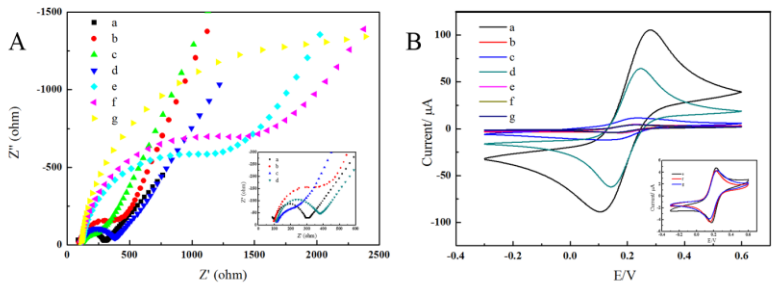

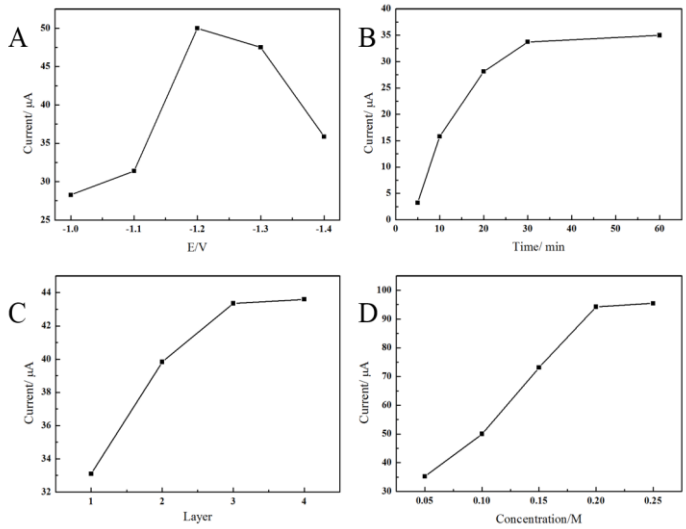

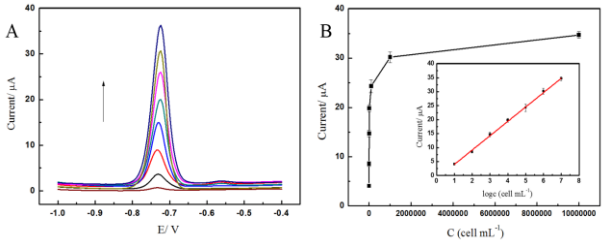

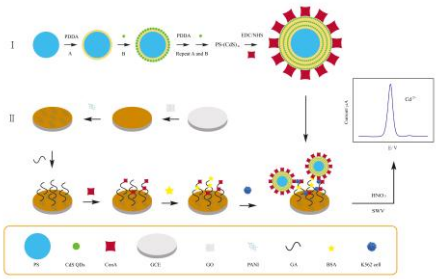

Highlights

- A signal amplification strategy for the fabrication of electrochemical biosensor was proposed based on multiple layer CdS QDs functionalized polystyrene microspheres(PS) as bioprobe and graphene oxide(GO) -polyaniline(PANI) composite as modified materials of capture eletrode.
- The resulting electrochemical biosensor was used to detect K562 cells with a lower detection limit of 3 cells mL^{-1} (S/N=3) and a wider linear range from 10 to 1.0×10^7 cells mL^{-1}.

- This sensor showed high specificity and sensitivity for mannosyl groups in different cancer cells including HeLa cells and Hct116 cells.
- This ultrasensitive electrochemical biosensor would push the progress in cancer early diagnosis and treatment due to its excellent analytical performance.